Proceedings of the 6th European VLBI Network Symposium
Ros, E., Porcas, R.W., Lobanov, A.P., & Zensus, J.A. (eds.)
June 25th-28th 2002, Bonn, Germany

Constraints on the circumnuclear absorber in NGC 1052 from Radio and X-ray observations

M. Kadler[1]*, E. Ros[1], J. Kerp[2], A. P. Lobanov[1], H. Falcke[1], and J. A. Zensus[1]

[1] Max-Planck-Institut für Radioastronomie, Auf dem Hügel 69, D-53121 Bonn, Germany
[2] Radioastronomisches Institut der Universität Bonn, Auf dem Hügel 71, D-53121 Bonn, Germany

Abstract. Multi-frequency studies of the pc-scale twin-jet in NGC 1052 have revealed the presence of a dense circumnuclear absorber obscuring the central engine. We analyze the brightness temperature distribution along the approaching, eastern pc-scale jet of NGC 1052 based on observational data obtained with the VLBA at 5, 8.4, 22 and 43 GHz. We present evidence for a geometry in which the central absorber covers also ~0.3 pc of the approaching jet in addition to the previously known obscuration of the receding jet. Further constraints on the properties of the circumnuclear absorber in NGC 1052 are obtained using the CHANDRA X-ray observatory. A rather moderate X-ray absorbing column density, substantially lower than previously published values, is derived from the nuclear X-ray spectrum. Imaging the extended X-ray emission reveals the presence of various jet-related X-ray emitting regions in NGC 1052: a bright compact core, unresolved knots in the jet structure, and an elongated, diffuse emission region whose spectrum can be described by a thermal model. We compare the spatial distribution of the diffuse X-ray emission on kpc-scales with the radio structure derived from a MERLIN observation and an optical image taken by the Hubble Space Telescope.

1. Introduction

NGC 1052 has become one of the most promising candidates for probing the physical properties of a circumnuclear absorber around a supermassive black hole predicted by the AGN standard model. The presence of such a central absorber in this elliptical galaxy is indicated by various observations of the pc-scale twin-jet using VLBI techniques, e.g. by Kellermann et al. (1999), Kameno et al. (2001), Kadler et al. (2002). Strong free-free absorption towards the receding western jet has been established by these authors. The obscuration of the jet by a circumnuclear disk or torus is sustained by the presence of water maser emission distributed along the western jet suggesting an interaction between the jet radiation field and circumnuclear, molecular matter (Claussen et al. 1998).

Evidence for the existence of a central absorber in NGC 1052 also comes from observations in the X-ray regime (Weaver et al. 1999, Guainazzi et al. 1999, Guainazzi et al. 2000). While free-free absorption at radio wavelengths is an indicator of ionized matter, absorption at X-ray frequencies can give information about neutral hydrogen (HI). The spectral analysis of the spatially unresolved X-ray spectrum suggests an obscuring neutral gas component with an absorbing column density of $N_{\rm H} \sim 10^{23}\,{\rm cm}^{-2}$. CHANDRA is the first X-ray imaging facility with an angular resolution high enough to separate the X-ray core and diffuse, extended emission. It is thus better suited to obtain an unpolluted nuclear spectrum than earlier missions.

In this work we use the high angular resolution of CHANDRA combined with VLBI observations in the radio regime to better constrain the physical properties of the central absorber in NGC 1052.

2. Evidence for free-free absorption towards the eastern jet

Figure 1 shows VLBA images of NGC 1052 in total intensity at 5, 8.4, 22 and 43 GHz obtained from our observations on December 28th 1998. In Kadler et al. (2002) we described the mapping and registration of the images. The spectral indices at the core of the western jet are larger than 2.5 indicating free-free absorption. The core position in both jets changes with frequency. The core-shift analysis suggests that the cores of both jets are covered by the central absorber and that the shift rates with frequency have also to be explained in terms of free-free absorption in conjunction with steep pressure gradients along both jets.

To clarify the geometry of the central absorber, we analyze the brightness temperature distribution along the approaching, eastern jet of NGC 1052. The brightness temperature associated with a circular Gaussian component is (e.g. Condon et al. 1982)

$$T_b = 1.22 \cdot 10^{12}{\rm K} \left(\frac{S_\nu}{\rm Jy}\right) \left(\frac{\nu}{\rm GHz}\right)^{-2} \left(\frac{\Theta}{\rm mas}\right)^{-2} \quad (1)$$

where S_ν is the flux density of the component, ν is the observing frequency and Θ is the FWHM of the model

* The author acknowledges partial support from the EC ICN RadioNET (Contract No. HPRI-CT-1999-40003).

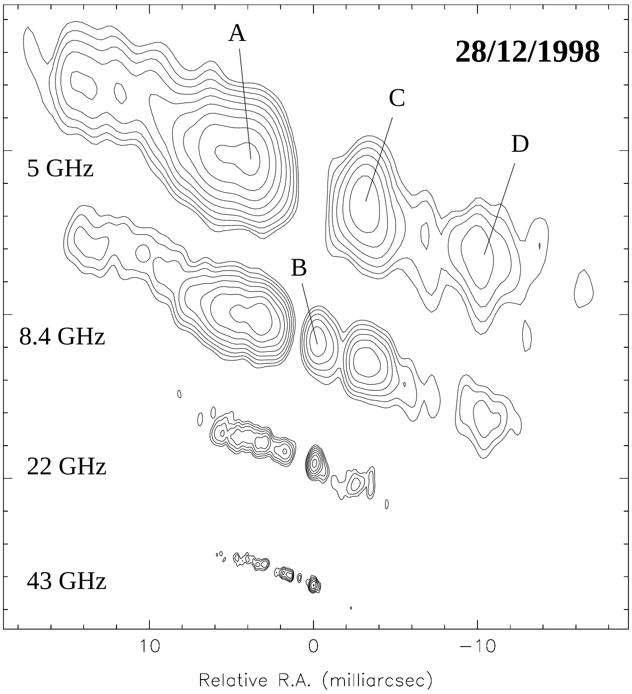

Fig. 1. The twin jet of NGC 1052 at 5, 8.4, 22 and 43 GHz at epoch 1998.99 observed with the VLBA (Kadler et al. 2002). The outer parts of both jets fade away towards higher frequencies, indicating optically thin synchrotron emission. The gap between both jets (presumably caused by the obscuring torus) becomes smaller at higher frequencies but stays prominent up to 43 GHz. There is no true core detectable, even at the smallest beam-size (corresponding to the highest resolution), at 43 GHz. Component B is totally absorbed at 5 GHz, indicating the presence of an obscuring torus, located in this region. A detailed analysis gives a spectral index well above 2.5, ruling out synchrotron self–absorption.

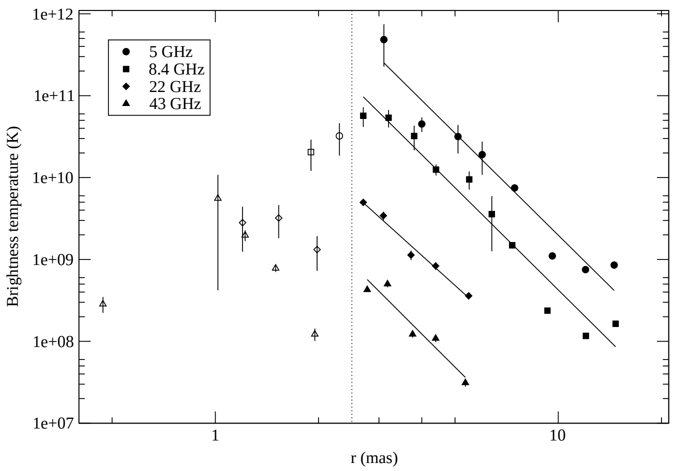

Fig. 2. Brightness temperature distribution along the eastern jet of NGC 1052. Farther out than ∼3 mas the data (solid symbols) can be approximated by a power-law of the form $T_b \propto r^{-4}$. The offsets between the four frequency-data sets reflects the frequency dependence of T_b. Inside a radius of 3 mas (∼0.3 pc) the brightness temperature of the jet is substantially reduced (open symbols). The location of the cutoff can be interpreted as the edge of the central absorber covering the core of the approaching, eastern jet.

component. In Figure 2, the brightness temperatures of the components along the eastern jet are plotted as a function of distance from the central engine, which is assumed to be located at the center between the innermost model components (see Kadler et al. 2002 for a detailed discussion). A conspicuous cutoff around 3 mas east of the center is present at all four frequencies[1]. Farther out, the data points can well be approximated by a power law of the form $\log T_b = A + B \cdot \log r$. A linear regression for the fit parameters gives at all four frequencies a $T_b \propto r^{-4}$ law. The frequency independence of the cutoff distance implies an external effect suggesting that at this position the influence of the nuclear absorber starts to affect substantially the jet and the brightness temperature of the components in it. This suggests the existence of an obscuring torus around the central engine of NGC 1052 with a sharp edge rather than a circumnuclear cloud system. In the case of free-free absorption, the observed flux density $S_{\nu,abs}$ should depend on the intrinsic flux density S_ν, the optical depth of the absorber τ_f and the observing frequency ν as

$$S_{\nu,abs} = S_\nu \cdot e^{-\tau_f} \quad . \tag{2}$$

Extrapolating the power–law dependence for each of the four frequency data sets to smaller distances (< 3 mas) we can calculate an optical depth for each data point that can explain the degradation of the brightness temperature with respect to the extrapolated value. The resulting values for τ_f are very similar and lie between 2 and 3. Assuming an absorbing path length of 0.3 pc (comparable to the extent of the absorbing region in the plane of the sky), the optical depth can be determined from (compare e.g. Rybicki & Lightman 1979)

$$\tau_f = 30 \cdot 10^{16}\, L\, T^{-1.35}\, \nu^{-2.1}\, n_{mean}^2 \tag{3}$$

$$\Rightarrow\ T^{-1.35}\, n_{mean}^2 = 3.33 \cdot 10^{-18}\, L^{-1} \tau_f\, \nu^{2.1} \tag{4}$$

with a length $L = \int dl$ and an average density n_{mean}. For $\tau_f \sim 2.5$ at $\nu = 22$ GHz and a temperature of $T = 10^4$ K, this gives a density of $n_{mean} = 6 \cdot 10^5\,\mathrm{cm}^{-3}$ and an absorbing column density of $5.6 \cdot 10^{22}\,\mathrm{cm}^{-2}$. This value is consistent with the implications of the X-ray observations of NGC 1052, which find a (model-dependent) column density of 10^{22}-$10^{23}\,\mathrm{cm}^{-2}$ (Weaver et al. 1999, Guainazzi et al. 1999, and section 4) towards the unresolved nuclear X-ray core.

3. The X-ray jet of NGC 1052

CHANDRA observed NGC 1052 on August 29/30, 2000[2]. During the 2342 sec. observation, the Advanced CCD Imaging Spectrometer (ACIS) Chip S3 was in focus of the

[1] At the distance of NGC 1052 ($D = 22.6$ Mpc) 1 mas corresponds to ∼0.11 pc (with H_0=65 km s^{-1} Mpc^{-1}).

[2] The CHANDRA data were taken from the public archive (`http://cxc.harvard.edu/cda/chaser.html`) and analyzed using standard methods within the software package CIAO 2.2. The observation was planned and scheduled by G. P. Garmire.

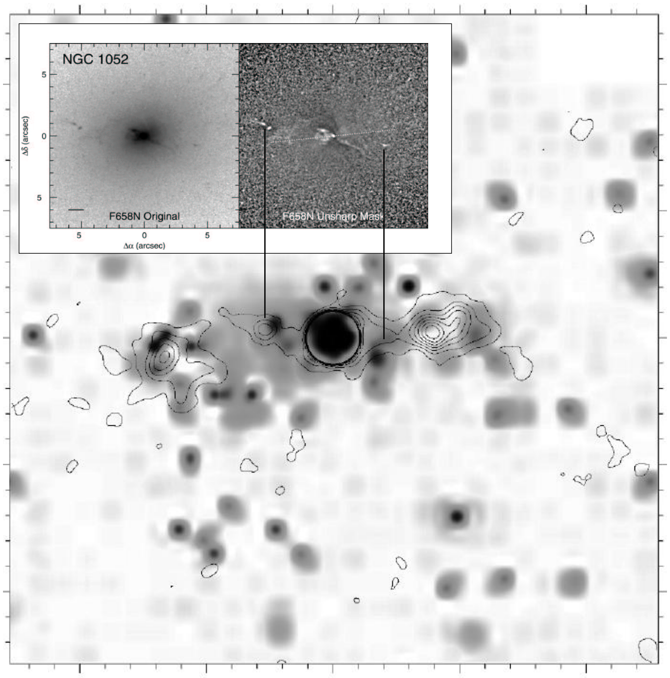

Fig. 3. The X-ray jet of NGC 1052 imaged by CHANDRA. The grey scale image has been smoothed to a resolution of 4″ within the CSMOOTH program, which is part of the CIAO software, to increase sensitivity. Each tick corresponds to 2″. The clipping level is 3σ. Overlaid are the radio contours from a 1.4GHz MERLIN map at epoch 1995.9 . The enclosed panel shows the HST image from Pogge et al. (2000) at the same scale. Two knots appear at the same positions as the corresponding X-ray features.

High Resolution Mirror Assembly (HRMA). The ACIS–S3 detector offers 0.″5 angular resolution as well as information on the X-ray source spectrum because of its intrinsic energy resolution.

The nucleus of NGC 1052 is the brightest X-ray source within the field of interest. During the rather short X-ray observation about 280 photons from the nucleus were detected. This value corresponds to a count rate of $0.12\,\mathrm{cts\,s^{-1}}$.

The CHANDRA image of NGC 1052 is shown in Figure 3. Strong X-ray emission from the AGN is seen in this image as well as diffuse extended emission well aligned with the radio jet, whose MERLIN image is superimposed in contours[3]. This is the first direct detection of the X-ray jet of NGC 1052.

Close to the nucleus a tentative correlation between radio and X-ray emission can be found while the synchrotron emission in the radio lobes tends to anti-correlate with the X-ray intensity distribution. East and west of the core, there are two X-ray emitting regions, coinciding with enhanced brightness regions in the radio regime, which can also be seen in an optical image, taken by the Hubble Space Telescope (Pogge et al. 2000). The X-rays from these knots might be produced in a very different physical process than the more diffuse, extended emission. Synchrotron or inverse Compton radiation could be responsible for their brightness over this large frequency range but the poor photon statistics prevented the derivation of spectra of either knot to test this hypothesis.

To constrain the emission process of the X-ray jet, we selected an annulus which excludes the nucleus itself but includes the whole area of the X-ray jet and fitted two different models to the jet–spectrum (see Figure 4): a Raymond and Smith plasma (Raymond & Smith 1977) and a simple power–law. We consider the power–law fit result of the X-ray jet as highly implausible, because of the extraordinary steep photon index of $\Gamma \geq 7$.

Because the radio as well as the X-ray jet are considered to be located deep inside the galaxy NGC 1052 itself, we have to determine the amount of photoelectric absorption distributed along the line of sight. Using the thermal source model, we find an attenuating column density of $N_{\mathrm{HI}} \simeq 3.5 \times 10^{21}\,\mathrm{cm}^{-2}$. This value is about an order of magnitude higher than the galactic foreground column density belonging to the Milky Way of $N_{\mathrm{HI}} = 2 \times 10^{20}\,\mathrm{cm}^{-2}$ (Hartmann & Burton 1997). We attribute this additional X-ray attenuation to weakly ionized gas located inside the galaxy itself. We derive a plasma temperature of $kT = (0.5 \pm 0.2)\,\mathrm{keV}$ for the diffuse X-ray jet emission.

4. The X-ray spectrum of the nucleus

The nuclear X-ray spectrum was extracted up to a diameter of 2 arcsec. Comparing both X-ray spectra in Figure 4 reveals the much softer X-ray emission of the jet. The bulk of the X-ray jet emission originates below $E < 2\,\mathrm{keV}$ while the X-ray spectrum of the nucleus has additional hard X-ray emission. ASCA as well as the ROSAT PSPC could not separate between the nucleus and the jet spatially but the soft X-ray emission of the jet was already detectable in terms of a soft excess of the X-ray spectrum in the PSPC data.

The soft X-ray emission below $E < 2\,\mathrm{keV}$ in the nuclear spectrum is at a comparable intensity level as the X-ray emission of the jet. Assuming that a fraction of the diffuse X-ray emission of the jet originates also in the extraction region of the nucleus, we used a hybrid model for the X-ray spectral approximation of the nuclear spectrum for the observed intensity distribution

$$I_{\mathrm{obs}} = (I_{\mathrm{jet}} + I_{\mathrm{nucleus}} \times e^{-\sigma \times N_H(\mathrm{torus})}) \times e^{-\sigma \times N_H(\mathrm{gal.})} \quad (5)$$

where I_{jet} is the X-ray spectrum of the jet and I_{nucleus} is the spectrum of the nucleus. The photoelectric absorption produced by the torus is represented in Eq. (5) by $e^{-\sigma \times N_H(\mathrm{torus})}$ while the X-ray absorption produced by the interstellar medium of the galaxy is $e^{-\sigma \times N_H(\mathrm{gal.})}$. We assumed a power–law type X-ray spectrum of the central X-ray source and fixed the plasma temperature of the

[3] The MERLIN data has been obtained from the public archive (`http://www.merlin.ac.uk`). The experiment was planned and scheduled by A. Pedlar. The map shown in contours in Figure 3 was produced applying standard methods using the program DIFMAP.

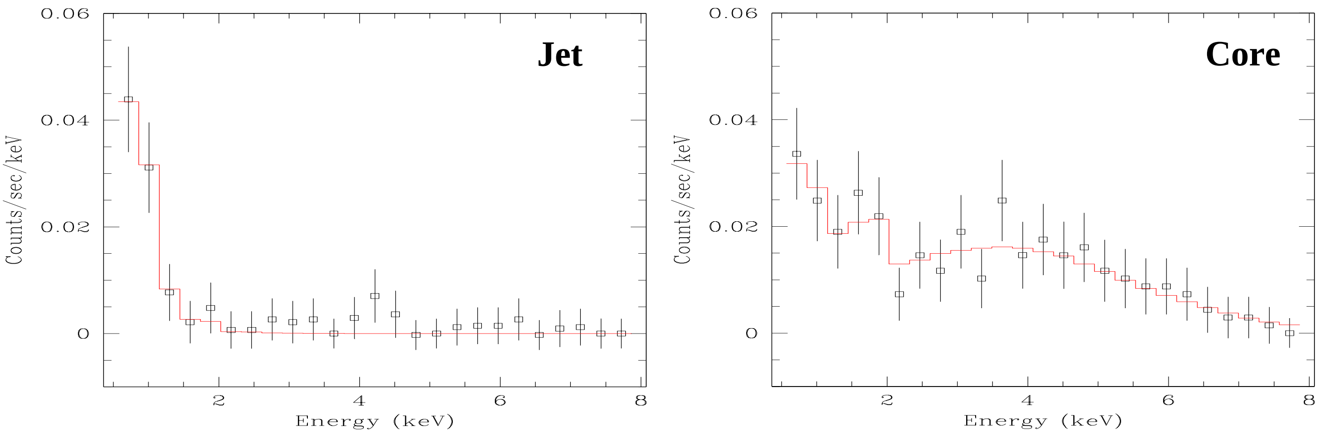

Fig. 4. X-ray spectrum of the jet (left panel) and core (right panel) of NGC 1052. The solid line indicates the best-fit model.

X-ray jet contribution as well as the foreground X-ray absorbing column densities to the values derived in section 3. The best fit values are: $N_{\rm H}(\rm torus) = 0.8^{+1.5}_{-0.60} \times 10^{23}\,\rm cm^{-2}$ and $\Gamma = 0.38^{0.31}_{-0.21}$. The absorbed X-ray flux is $F_{\rm X}(0.3 - 8.0\,\rm keV) = (4.3 \pm 1.4) \times 10^{-12}\,\rm erg\,s^{-1}\,cm^{-2}$.

The derived $N_{\rm H}(\rm torus)$ is rather low. Data of other X-ray observatories imply much higher values for both, the $N_{\rm H}(\rm torus)$ as well as Γ (Weaver et al. 1999, Guainazzi et al. 1999, Guainazzi et al. 2000) but these high torus column densities are not supported by the CHANDRA data. We assume that the apparent discrepancy between the CHANDRA data and previous X-ray observations concerning the photon index is due to the pile–up degradation ($\sim$ 30 %) of the CHANDRA data. The nuclear X-ray spectrum might appear flatter than expected, because of the artificial hardening of the X-ray spectrum introduced by the pile–up effect. Taking this into consideration, our results are consistent with the analysis of Weaver et al. (1999) who fitted the combined ROSAT and ASCA data – both are not affected by the pile–up – and derived in general steeper X-ray photon indices using a variety of models. The determined absorbing column density, however, is not so sensitive to the pile–up effect.

We tried to substitute $I_{\rm nucleus}$ from a power–law to a thermal bremsstrahlung model. No approximation was feasible. In all cases the temperature values exceed the upper temperature boundary of 1 MeV.

5. Summary

The CHANDRA data provide for the first time direct evidence for an X-ray jet in NGC 1052 perfectly correlated in extent with the well studied radio jet. The X-ray jet can be approximated best with thermal X-ray emission of a plasma with $kT = 0.5\,\rm keV$. This temperature is consistent with the thermal component found earlier by Weaver et al. (1999) using ASCA and ROSAT data. Its unabsorbed flux is $F_{\rm X-ray\,jet}(0.3 - 8.0\,\rm keV) = (1.7 \pm 0.8) \times 10^{-13}\,\rm erg\,s^{-1}\,cm^{-2}$, only 2% of the X-ray emission of the nucleus. Because of the strong pile–up degradation of the CHANDRA data, no firm conclusions on the X-ray spectrum of the nucleus can be deduced. The absorbing column density of ionized material towards the approaching VLBI–jet derived from the brightness temperature distribution is of the order of $\sim 6{\cdot}10^{22}\,\rm cm^{-2}$. This is in a good agreement with the absorbing column density of neutral hydrogen ($0.8^{+1.5}_{-0.60} \cdot 10^{23}\,\rm cm^{-2}$) derived from X-ray spectroscopy of the compact X-ray core of NGC 1052.

Acknowledgements. MERLIN is a National Facility operated by the University of Manchester at Jodrell Bank Observatory on behalf of PPARC. The VLBA is operated by the National Radio Astronomy Observatory (NRAO), a facility of the National Science Foundation operated under cooperative agreement by Associated Universities, Inc. The CHANDRA Data Archive (CDA) is part of the CHANDRA X-Ray Observatory Science Center (CXC) which is operated for NASA by the Smithsonian Astrophysical Observatory.

References

Claussen, M. J., Diamond, P. J., Braatz, J. A., Wilson, A. S., Henkel, C. 1998, AJ, 500, 129
Condon, J. J., Condon, M. A., Gisler, G., Puschell, J. J. 1982, ApJ, 252, 102
Guainazzi, M., Antonelli, L. A. 1999, Monthly Not. Roy. Astron. Soc, 304, 15
Guainazzi, M., Oosterbroek, T., Antonelli, L. A., Matt, G. 2000, A&A, 364, 80
Hartmann, D., Burton, W. B. 1997, in Atlas of galactic neutral hydrogen, Cambridge; New York: Cambridge University Press
Kadler, M., Ros, E., Zensus, J. A., Lobanov, A. P., Falcke, H. 2002, SRT Conference Proceedings, Vol. 1, in press (astro-ph/0204054)
Kameno, S., Sawada-Satoh, S., Inoue, M., Shen, Z., Wajima, K. 2001, Publ. Astron. Soc. Japan, 53, 169
Kellermann, K. I., Vermeulen, R. C., Cohen, M. H., Zensus, J. A. 1999, American Astronomical Society Meeting, Vol. 194, #20.02
Pogge, R. W., Maoz, D., Ho, L. C., Eracleous, M. 2000, AJ, 532, 323
Raymond, J. C., Smith, B. W. 1977, ApJS, 35, 419
Rybicki, G. B., Lightman, A. P. 1979, Radiative Processes in Astrophysics, New York: Wiley-Interscience
Weaver, K. A., Wilson, A. S., Henkel, C., Braatz, J. A. 1999, AJ, 520, 130